

Supporting Information

Nitrogen-doped carbon dots for efficient deep-blue light-emitting diodes with CIE closely approaching the HDTV standard color Rec.BT.709

Peng Huang,^{†a} Ming-Zhu Li,^{†a} Chun-Fa Wen,^a Hang-Yue Zhou,^b Jing-Xin Jian,^{*a} and Qing-Xiao Tong^{*a}

^aDepartment of Chemistry, Key Laboratory for Preparation and Application of Ordered Structural Material of Guangdong Province, and Guangdong Provincial Key Laboratory of Marine Disaster Prediction and Prevention, Shantou University, Shantou, Guangdong, 515063, China.

^bSchool of Chemistry & Materials Engineering, Xinxiang University, Xinxiang, Henan, 453003 China.

[†] The two authors contribute equally to this work.

Synthesis of N-doped CDs.

High concentration N-doped CDs were synthesized by the solvothermal method. Accordingly, 0.15 g of DL-malic acid was mixed with 0.15 g o-phenylenediamine. Then, the reaction mixture was dissolved in 10 mL ethanol by ultrasound at 50 °C for 30 min followed by transfer into a 25 mL high-pressure reactor and was moved into a Muffle furnace to heat at 180 °C for 360 min. After the reaction, the solution was cooled to room temperature.

The purification of CDs crude product is processed through silica gel column chromatography, since this kind of purification could separate products with different solubility and polarity from each other. Dichloromethane and methanol were selected as eluent according to the polarity of the solution. The byproducts with weak fluorescence and no fluorescence properties were verified by thin layer chromatography and irradiation with 365 nm UV lamp. After the silica gel column chromatography, a purified N-doped CDs sample was obtained by rotary cooking and vacuum sampling.

Fabrication of CLED Devices.

The ITO glass was cleaned with Deacon 90 detergent to remove the surface of glue, oil, microorganism and other impurities. Then it was heat under ultrasonic with alcohol and deionized water for 30 min and finally it was dried by blowing nitrogen. The clean ITO substrate was placed in the oven with clean tweezers and dried at 120 °C for 2 hours. After that, the ITO substrate irradiated for 30 min by using ultraviolet ozone plasma and then transferred into glove box. The hole injection layer of poly(3,4-ethylenedioxythiophene): poly(styrenesulfonate) (PEDOT:PSS) was spin-coated at 5500 rpm for 50 s on ITO substrate, then dried at 150 °C for 30 min. Subsequently, poly(9,9-dioctylfluorene-coN-(4-(3-methylpropyl)) diphenylamine (TFB) was dissolved in chlorobenzene (5 mg mL⁻¹), spin-coated on the top of PEDOT:PSS layer at 5,000 rpm for 50 s, and annealed at 150 °C for 30 min. The emitter layer of CDs was blended with poly(N-vinyl carbazole) (PVK) at different concentrations and spin-coated at 2500 rpm for 30 s on the top of TFB layer, followed by annealing at 120 °C for 10 min. Finally, the device was transferred to a vacuum chamber, and 1,3,5-Tris (N-

phenylbenzimidazol-2-yl) (TPBi) (60 nm) and LiF/Al electrodes (1 nm/100 nm) were deposited using an Organic Small Molecule evaporation system through a shadow mask under a high vacuum of less than 10^{-4} Pa. The luminescence spectra, CIE coordinate, EQE value, luminance and current density of the devices were measured by PR650 spectral photometer and Keithley 2400 digital source meter.

Characterizations.

The PL spectra was determined by Hitachi F7000 luminescence spectrophotometer. The PLQY of CDs were determined on the Quantaaurus-QY Absolute PL quantum yield spectrometer (Hamamatsu C11347-11), with integrating spheres (Spectralon) detection. Hamamatsu C11347-11 includes an excitation light source of a xenon lamp, monochromators that provides monochromatic light with a certain intensity, an integration sphere with optional nitrogen gas flow, and a multichannel detector capable of simultaneous multi-wavelength measurement. Fluorescence standard solutions were measured with Absolute PL Quantum Yield Measurement System, which shows excellent agreement with the values given in the literature, proving high reliability at different wavelength. JEM-F200 TEM instrument was used to investigate the morphologies of CDs. Fourier transform infrared (FTIR) spectroscopy was performed on a Nicolet iS50 spectrometer. XPS measurements were measured on the Thermo ESCALAB 250Xi Multifunctional imaging electron spectrometer. The nuclear magnetic resonance spectra were recorded on the Bruker Ascend™ 400 MHz NMR spectrometer with tetramethylsilane (TMS) as an internal standard.

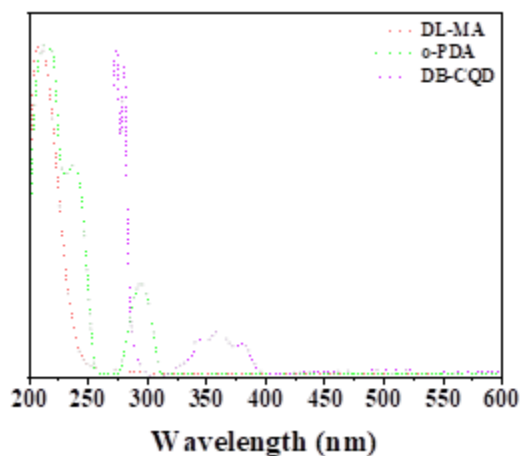


Fig. S1 UV-vis absorption spectra of deep blue CDs and precursors of DL-MA and o-PDA in ethanol.

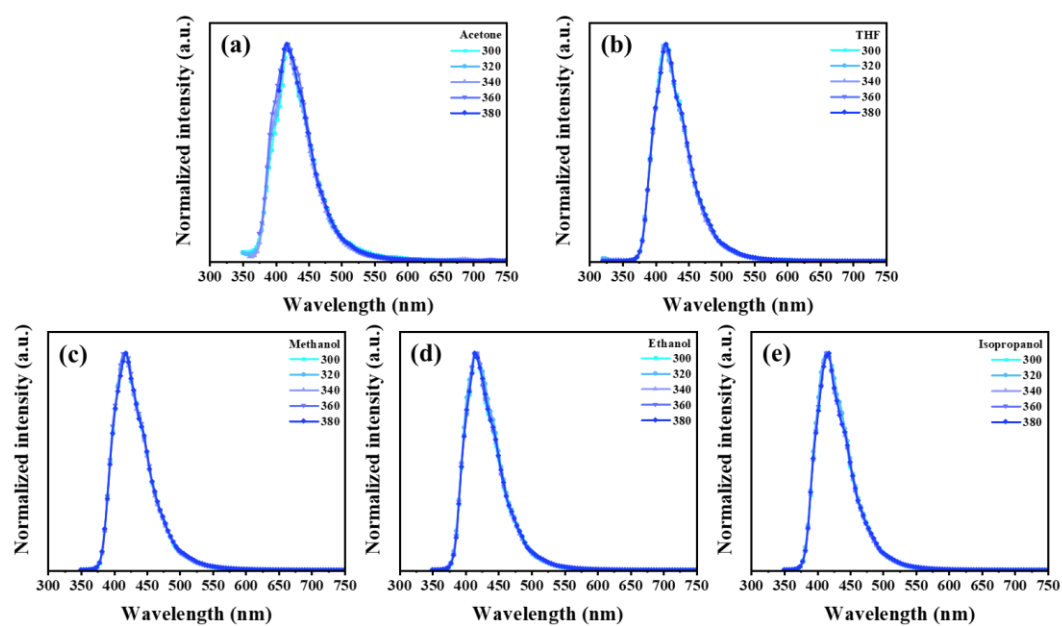


Fig. S2 PL spectra of N-doped CDs under different excitations in the solvents of acetone (a), tetrahydrofuran (THF) (b), methanol (c), ethanol (d) and isopropanol (IPA) (e).

Table S1 PLQY of CDs at different N doping concentrations

Materials examples	N (%)	PLQY (%)	Reference
Asn N-PDA-B-CD	1.81	18.0	1
Asn N-PDA-R-CD	2.20	19.0	
Asn N-PDA-O-CD	5.36	54.0	
Asn N-PDA-G-CD	8.51	74.0	
o-BN-CDs	2.7.0	31.1	2
BNQD	3.38	32.2	3
N-doped CDs	9.80	60.0	This work

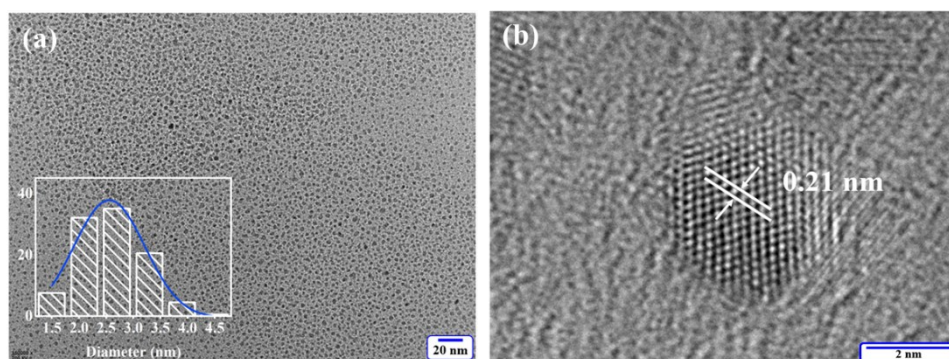


Fig. S3 TEM image (scale bar: 20 nm), corresponding statistical size distributions of CDs. (b) High-resolution TEM image (scale bar: 2 nm) of CDs.

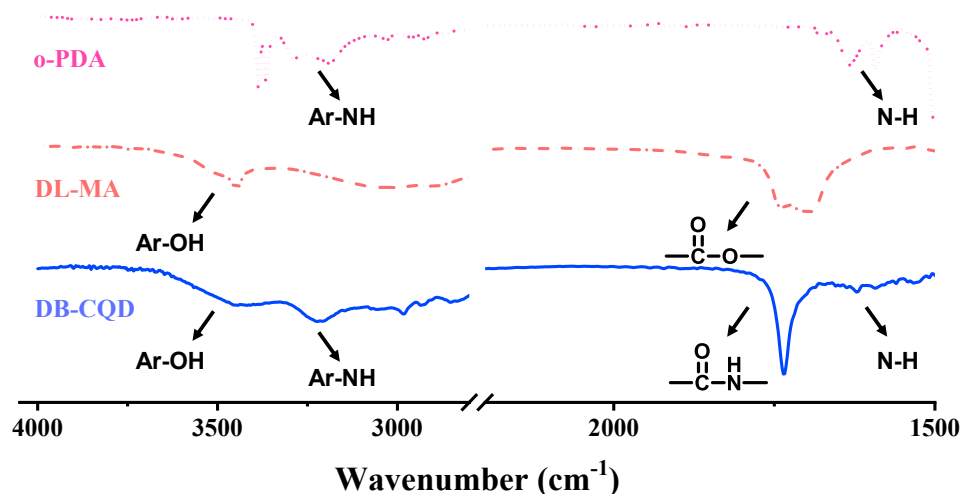


Fig. S4 FTIR spectra of o-PDA, DL-MA and CDs.

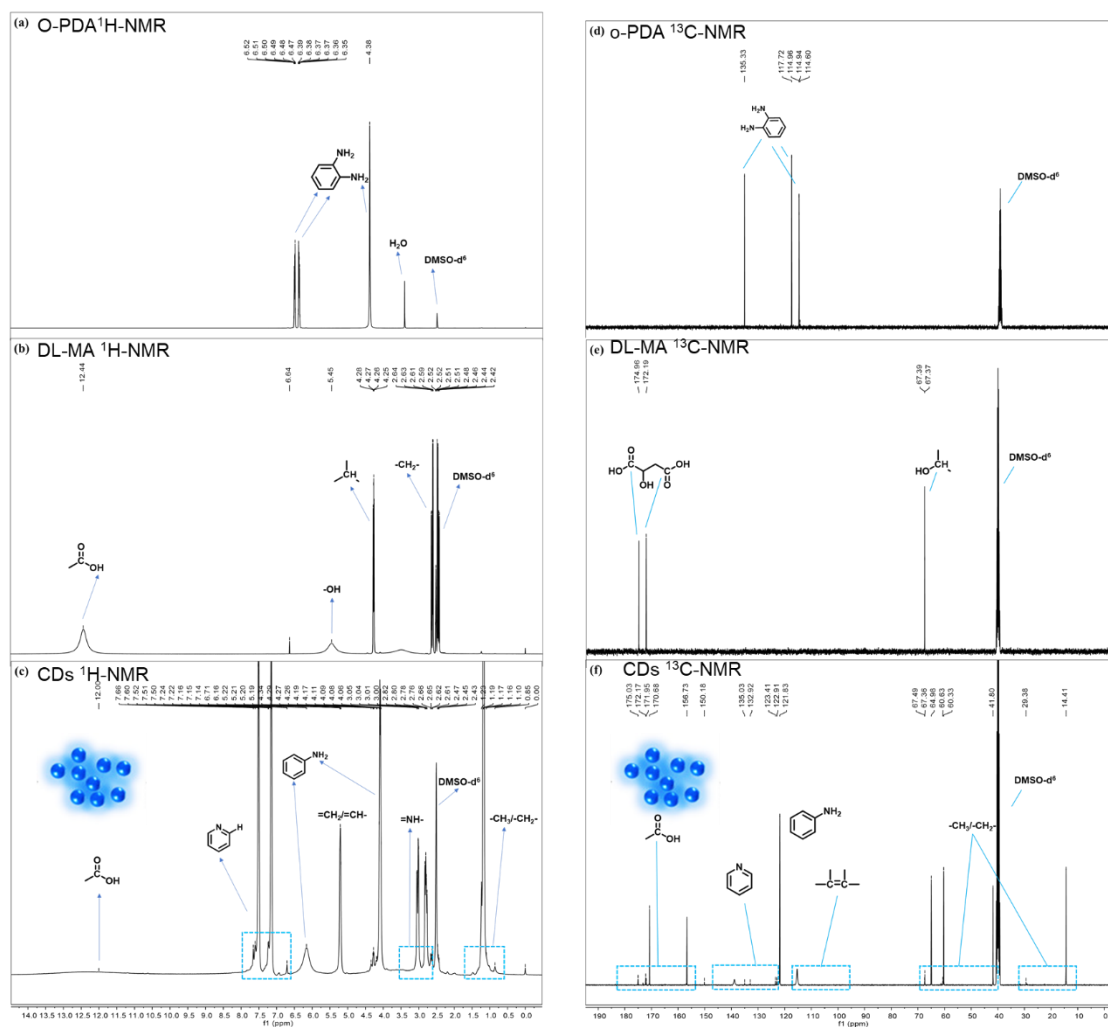


Fig. S5 ^1H NMR spectra of o-PDA (a), DL-MA (b), N-doped CDs (c) and ^{13}C NMR spectra of o-PDA (d), DL-MA (e), N-doped CDs (f).

Table S2 XPS data analyses of N-doped CDs.

C 1s				N 1s			O 1s	
C=C	C-N	C-O	O-C=O	Pyridine N	Graphitic N	N-H	C=O	C-O
26.7%	24.8%	13.8%	6.40%	2.10%	4.60%	3.10%	9.80%	8.70%

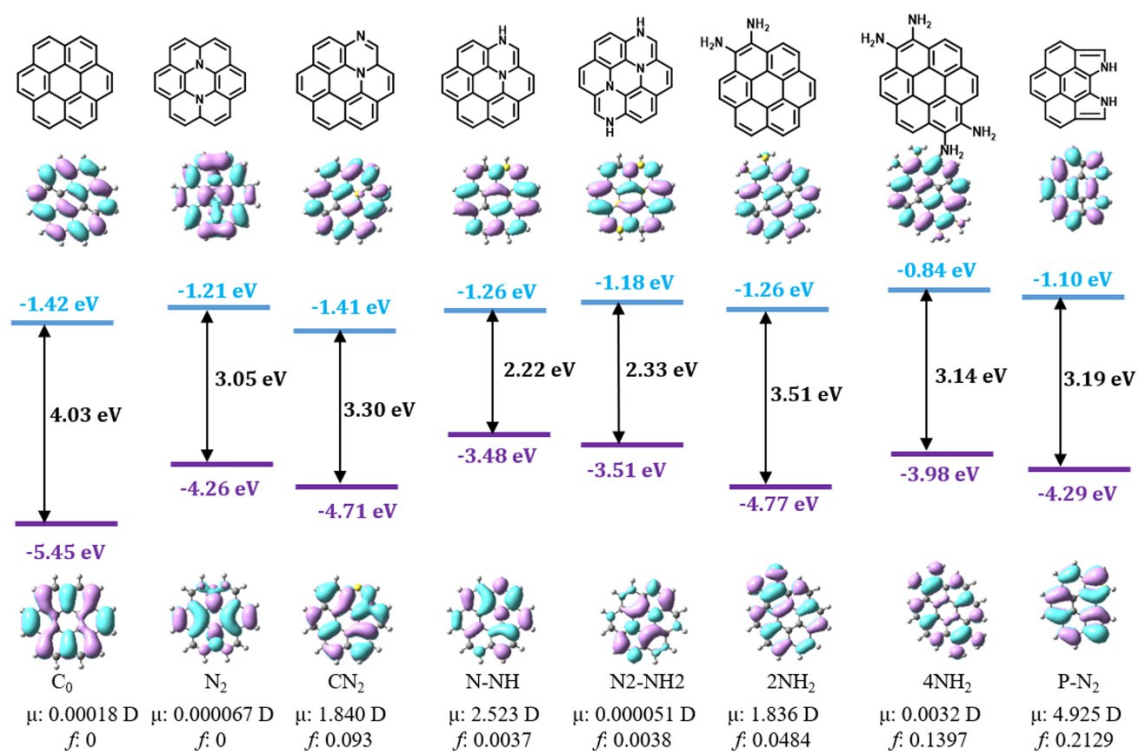
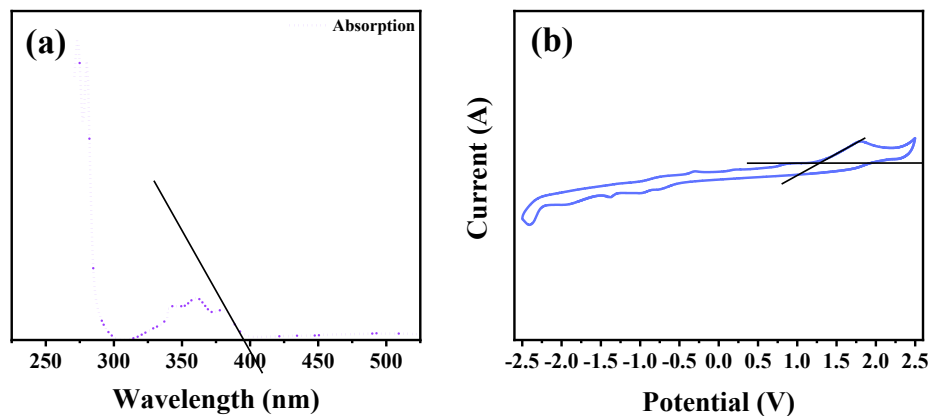


Fig. S6 DFT models of CDs with optimized structures and related band levels, dipole moment (μ) and oscillator strength (f) parameters



$$E_{\text{HOMO}}(\text{DB-CQD}) = - [1.29 - 0.36 + 4.8] = -5.73 \text{ eV}$$

$$\lambda_{\text{abs, onset}}(\text{DB-CQD}) = 395 \text{ nm}; E_{\text{g}}(\text{DB-CQD}) = 1240/395 = 3.14 \text{ eV}$$

$$E_{\text{LUMO}}(\text{DB-CQD}) = -2.59 \text{ eV}$$

Fig. S7 UV-vis absorption (a) and cyclic voltammetry (b) of N-doped CDs.

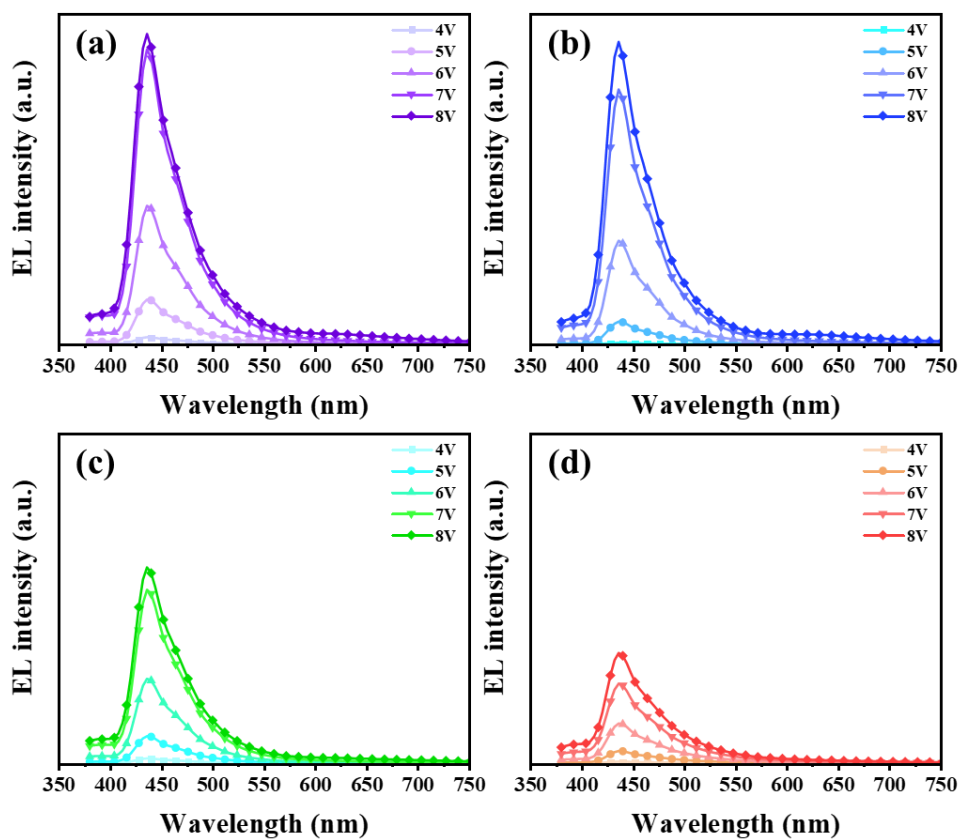


Fig. S8 EL emission spectra of (a) 4%-CLED, (b) 8%-CLED, (c) 12%-CLED and (d) 16%-CLED at different voltages.

Table S3 PLQY of 4%, 8%, 12%, and 16% CQDs/PVK films.

CDs doping [%]	4	8	12	16
PLQY [%]	17.6	18.5	12.3	8.5

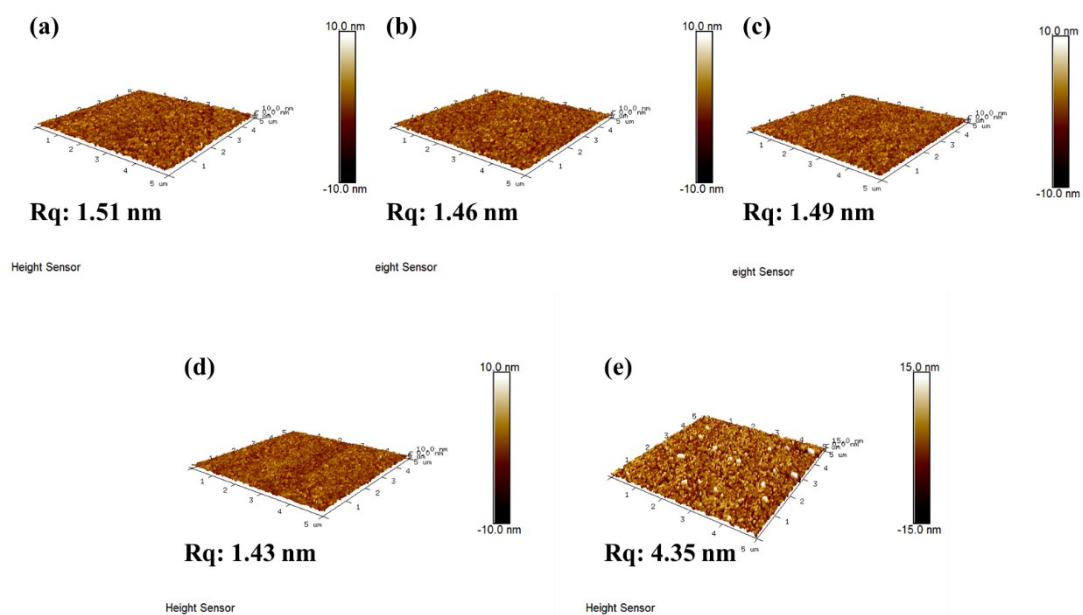


Fig. S9 AFM images of CDs/PVK and CDs films with different doping concentrations of CDs. 4% CDs/PVK (a), 8% CDs/PVK (b), 12% CDs/PVK (c), 16% CDs/PVK (d) and pure CDs (e).



Fig. S10 Image of 8%-CLED at work.

Table S4 The EL performance at different doping concentrations CLED.

Doping [%]	CIE [x, y]	V _(on) [V]	L _(max) [cd m ⁻²]	EQE ^[a] (max)/(100)	Efficiency roll-off ^[b]
4%	(0.16, 0.08)	3.5	1322.0	1.09/1.03	6.42
8%	(0.16, 0.08)	3.5	1155.0	1.74/1.54	11.49
12%	(0.16, 0.08)	3.5	445.4	0.98/0.80	18.36
16%	(0.16, 0.11)	3.5	276.8	0.62/0.50	19.35

[a] External quantum efficiencies of maxima and at luminance of 100 cd m⁻².

[b] Efficiency roll-offs at luminance of 100 cd m⁻².

Reference:

- 1 Y. X. Zheng, K. Arkin, J. W. Hao, S. Y. Zhang, W. Guan, L. L. Wang, Y. N. Guo, Q. K. Shang, *Adv. Optical Mater.*, 2021, **9**, 2100688.
- 2 J. Wang, Q. Li, J. Zheng, Y. Yang, X. Liu, B. Xu, *ACS Sustain. Chem. Eng.*, 2021, **9**, 2224-2236.
- 3 Y. Ding, P. He, S. Li, B. Chang, S. Zhang, Z. Wang, J. Chen, J. Yu, S. Wu, H. Zeng, L. Tao, *ACS Nano*, 2021, **15**, 14610-14617.